Available online at www.sciencedirect.com
ScienceDirect
Energy and Buildings 39 (2007) 128–135
ENERGY and BUILDINGS
www.elsevier.com/locate/enbuild

Air flow and thermal efficiency characteristics in solar chimneys and Trombe Walls

S.A.M. Burek [a,*], A. Habeb [b]

[a] Glasgow Caledonian University, Cowcaddens Road, Glasgow G4 0BA, Scotland, UK
[b] Faculty of Engineering and Technology, Sebha University, Brack Alshty, P.O. Box 68, Libya

Received 4 December 2005; received in revised form 20 March 2006; accepted 15 April 2006

Abstract

This paper reports on an experimental investigation into heat transfer and mass flow in thermosyphoning air heaters, such as solar chimneys and Trombe Walls. The test rig comprised a vertical open-ended channel with closed sides, resembling a solar collector or solar chimney approximately 1 m^2. Close control of the heat input was achieved by using an electrical heating mat—steady-state heat inputs ranged from 200 to 1000 W, and the channel depth was varied between 20 and 110 mm. Temperatures were recorded throughout the test rig, as was the air velocity. The principal results from the data showed:

- The mass flow rate through the channel was a function of both the heat input and the channel depth:
  $m \propto Q_i^{0.572}$

  and
  $m \propto s^{0.712}$
- The thermal efficiency of the system (as a solar collector) was a function of the heat input, and not dependent on the channel depth:
  $\eta \propto Q_i^{0.298}$

Correlations are given in dimensionless forms.

Keywords: Natural convection; Trombe Walls; Solar chimneys; Experiment; Thermosyphoning air panel

1. Introduction

Trombe Walls and solar chimneys are passive building elements which rely on solar-induced buoyancy-driven convection. In contrast to fan-driven (forced) convection, buoyancy-driven (natural) convection components are more difficult to analyse and it is more difficult to predict their performance, not least because mass flow depends on the heat input and also on the geometry of the system, and therefore it is not easily controlled.

Buoyancy-driven convection from a single vertical plate has been studied extensively, but in Trombe Walls and solar chimneys the flow is constrained within a vertical channel. Elenbaas [1] reported one of the first detailed investigations of buoyancy-driven convection of air between parallel plates. His experiments were performed on a small-scale test rig, with plates up to 24 cm high. Subsequent investigators used air (for example [2–7]) and water (for example [8]) to study various aspects of this type of system. However, most of these studies were done under conditions more applicable to electronics applications, for example: plate sizes were small, typically up to 30 cm high; in some cases the vertical surfaces were configured to have a uniform wall temperature (UWT), as opposed to a uniform heat flux (UHF); in some cases the channels were open-sided, as might be expected in a rack of printed-circuit boards; and mostly the experiments were constrained to have symmetrical heating or one adiabatic surface.

* Corresponding author. Tel.: +44 141 331 3897; fax: +44 141 331 3639.
E-mail address: s.burek@gcal.ac.uk (S.A.M. Burek).

0378-7788/$ – see front matter © 2006 Elsevier B.V. All rights reserved.
doi:10.1016/j.enbuild.2006.04.015

Nomenclature

a	regression constant: see Eq. (2)
A_x	cross-sectional area of the channel (m^2)
b	regression constant: see Eq. (2)
c	regression constant: see Eq. (2)
c_p	specific heat capacity of air (J/kg °C)
F_R	heat removal factor
g	acceleration due to gravity (=9.81 m/s^2)
H	height (length) of the channel (m)
I	incident solar radiation (W/m^2)
k	thermal conductivity of air (W/m °C)
m	air mass flow rate (kg/s)
Pr	Prandtl number
q_i	heat input per unit area (W/m^2)
Q_i	heat input (W)
Q_o	heat gain by the air in the channel (heat output) (W)
Ra^*	modified Rayleigh number: see Eq. (4)
$Re(s)$	Reynolds number based on channel depth: see Eq. (3)
s	channel depth (m)
T_a	ambient temperature (°C)
T_i	inlet temperature (°C)
T_o	outlet temperature (°C)
u	air bulk velocity (m/s)
U_L	overall heat loss coefficient (W/m^2 °C)

Greek symbols

β	thermal expansion coefficient (K^{-1})
η	thermal efficiency
ν	kinematic viscosity (m^2/s)
ρ	air density (kg/m^3)
$\tau\alpha$	transmittance–absorbtance product

In parallel with this experimentation, various analytical techniques were being developed. For example, Bodoia and Osterle [9] reported a model which was in good agreement in the results presented in [1], and since then, other models have been presented of increasing sophistication (for example [2,10–12]). Mostly, these models did not differentiate between solar applications and electronics applications, treating the problem as a phenomenon of natural convection between parallel plates, and in particular ignoring the effects of radiative heat transfer and heat losses through glazed walls.

However, Akbari and Borgers [13] and Borgers and Akbari [14] developed models which recognised the particular nature of Trombe Walls, namely that the channel is asymmetrically heated, and that heat losses occur through the glazing. Other models based on boundary-layer analysis followed, for example [15–18]. Some researchers coupled other parts of the building into their models [19,20].

Ong and co-workers [21,22] developed a simplified thermal network, based on the bulk properties of the flow, rather than on a detailed study of the behaviour of the boundary layer. Other simplified thermal networks and lumped-parameter models have been developed to predict the diurnal performance of a solar chimney or Trombe Wall—in particular, Balocco [23] and Infield et al. [24] used experimental or monitored data to validate their models. Bansal et al. [25] described a model of a Trombe Wall based on Fourier series analysis, used to predict the diurnal performance.

A variety of experiments have been reported, using test cells or real buildings under outdoor conditions. For example: Hirunlabh et al. [26] monitored the ventilation due to a thermosyphoning air panel in Bangkok; Sandbergh and Moshfegh [27] presented temperature data for flow in a ventilated PV channel, comparing two different geometries for the outlet from the channel; and Afonso and Oliveira [28] studied air flow through a roof mounted solar chimney, using a tracer-gas technique. Whilst these types of experiments are necessary and important, they report on the performance of test rigs in very specific and uncontrolled conditions.

Hocevar and Casperson [29] reported some early measurements of velocity and temperature profiles in a Trombe Wall channel, but there have been relatively few reports of detailed measurements under controlled conditions and on a scale which represents Trombe Walls and solar chimneys, which could be used to characterise the airflow within the channel on this scale. Bouchair [30] reported results from a solar chimney test rig, with channel depths ranging from 100 to 500 mm, for a symmetrically heated channel. La Pica et al. [31] recorded data from a channel 2.6 m high. The channel was heated from one side using an electrical heating mat (the 'absorber plate' in terms of a Trombe Wall), and the other surface (the 'cover') was silvered to reduce heat losses. The airflow, and temperatures at various points on the plate and in the channel, were measured, with different channel depths ranging from 75 to 170 mm and heat inputs from 48 to 317 W/m^2. Chen et al. [32] reported on a similar set of experiments, using a 1.5 m high rig, with a Plexiglas cover. Heat inputs ranged from 200 to 600 W/m^2, and channel depths from 100 to 600 mm.

The present paper reports on a set of experiments conducted to measure the airflow and temperature profiles in a test rig designed to simulate the essential features of a Trombe Wall or solar chimney. The results are presented in dimensionless form, based on parameters which are either known or controllable. The results are compared with those of the previous investigation reported by La Pica et al. [31]. The aim is to present data which can be used to characterise the airflow and temperature within large-scale thermosyphoning systems, such as Trombe Walls and solar chimneys, on a similar basis to those which have been collected for small-scale applications.

2. Experimental set-up

The test rig comprised a vertical channel, open at the top and bottom, and enclosed at the sides. The dimensions of the channel were 102.5 cm high and 92.5 cm wide (area 0.948 m^2). The depth of the channel could be altered, ranging from 20 to 110 mm.

The channel was constructed to resemble the essential workings of a solar collector. Thus, it had a transparent cover

(made of Perspex—polymethyl methacrylate), and an aluminium 'absorber plate', painted matt black. The heat input was provided by an electrical heating mat behind the absorber plate. Compared with testing a system outside in the sun or using artificial lighting to simulate the solar input, this arrangement was much simpler to control, and given the objectives of the experiment, it was considered adequate. A 100 mm layer of insulation was applied behind the heating mat, to ensure that stray heat losses were minimised—see Fig. 1.

The test rig was instrumented to measure temperature profiles across the depth at the vertical centre-line of the channel. Fine (0.2 mm diameter) thermocouples were inserted at six positions along the height of the channel. At each position there were four thermocouples in the air channel, one attached to the heating ('absorber') plate, and one to the cover—a total of 36 thermocouples. The thermocouples in the air stream were placed centrally inside lightweight radiation shields, designed specifically to reduce as far as possible any effects on the airflow or temperatures within the channel. A further thermocouple was used to measure ambient temperature.

Air velocity was measured using a sensitive hot-bead anemometer (Prosser Scientific Instruments, model 521L), located at the centre of the channel, approximately 50 mm from the bottom. This was calibrated down to 0.2 m/s, but earlier studies suggest that lower readings were self-consistent and could be used with care [33].

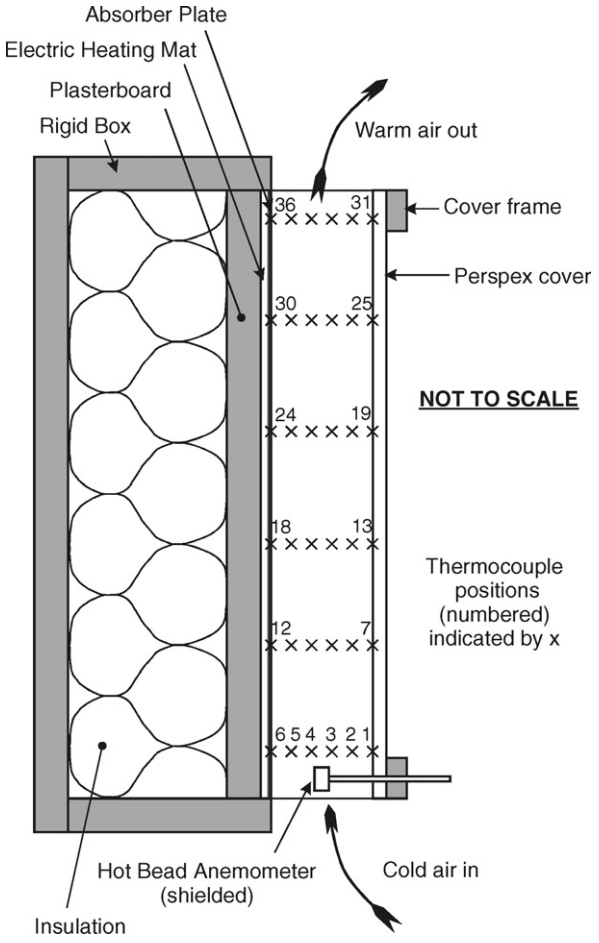

Fig. 1. Schematic diagram of the test rig (not to scale).

3. Experimental procedure

The channel depth could be varied, using spacer blocks, to 20, 40, 60, 80, 100 and 110 mm. For each of these channel depths, five heat inputs were studied: 200–1000 W, in 200 W steps, i.e., a total of 30 different test runs. Each test run started from cold (ambient temperature). The electric heating mat was switched on and the power input was adjusted to the required level (measured by a wattmeter Feedback Electronic Company, model EW604). Temperatures from all 37 thermocouples and velocity readings were recorded, using a Solartron Scorpio data logger. The power input to the heating mat was monitored, and was found to be constant throughout each test run, as the test rig heated up. It took typically 3–4 hours after the start of a test run to achieve steady state—this paper is concerned only with the final steady-state conditions for each test run.

In addition to the temperature and velocity readings, recorded during the heating-up period, the velocity profile of the airflow was determined when steady state had been reached, by measuring the airflow at points across the channel depth at the bottom of the channel. Velocity readings were taken at intervals of between 2 and 5 mm across the channel (depending on the channel depth): 60 readings at each point at 1-s intervals.

More details of the experimental equipment and procedures are presented by Habeb [34].

4. Initial observations

The following observations were made:

- In all cases, the temperature profiles of the air, as measured across the channel, were fairly flat across the main part of the channel. A typical temperature profile across the channel is shown in Fig. 2. This is similar to data reported by Chen et al. [32].

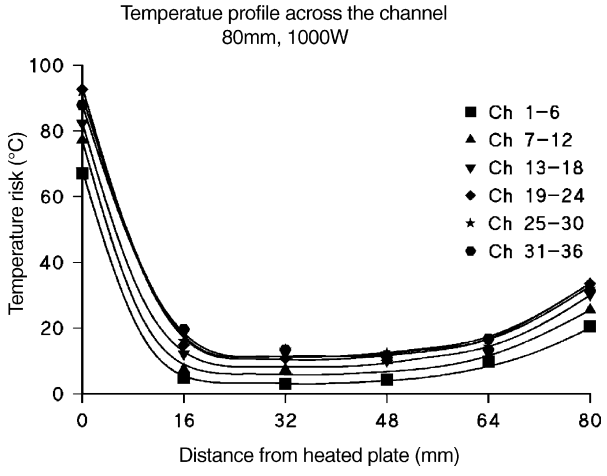

Fig. 2. Typical profile of temperatures across the channel depth at different heights: data shown for 80 mm channel depth, 1000 W input.

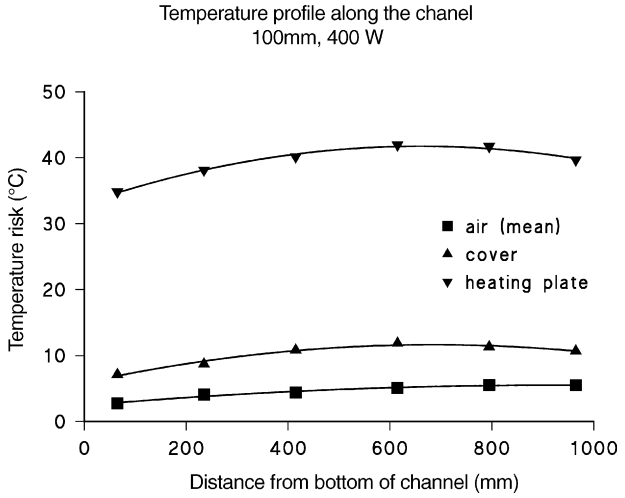

Fig. 3. Typical profile of temperatures along the channel height: data shown for 100 mm channel depth, 400 W input.

- In each case, the cover temperature was greater than the air temperature (but less than the plate temperature)—see Fig. 2. Similar observations have been made by previous workers [31,32,35,36], which can be attributed to radiation heat transfer from the heated plate to the cover. Sandberg and Moshfegh [27] suggested that as much as 40% of the heat absorbed by the absorber plate in a solar collector can be transferred by radiation to the cover. Many solar collectors make use of selective surface materials to reduce the radiated heat from the absorber plate, but this also suggests that low-emissivity materials, as often used in glazing in buildings, might be useful to reduce the radiation absorbed by the cover.
- In many cases, temperatures at the highest position were lower than the temperatures below them, i.e., the temperature fell towards the top of the channel. This applies particularly to the heating plate and the cover, and can be seen clearly in Fig. 3. This is contrary to what simple theory suggests, whereby the temperature should rise exponentially towards an asymptote (see, for example [37]). Other workers [31,32,36,38] have also observed this phenomenon, but the cause is not entirely clear—possibly due to radiation from the top of the plate directly to the surroundings, where the view factor is greater than in the middle of the plate; or a result of a changing boundary-layer regime [32].
- Velocity profiles, as measured across the bottom of the channel, were generally flat across most of the width of the channel. This indicates an undeveloped velocity profile, with very thin boundary layers at this point. This may be expected, as is assumed by many numerical analyses of this type of system.

As a result of these observations, the following assumptions are made in the analysis below:

- The temperature of the air in the channel at any height is taken as the mean of the measured air temperatures at that height.
- The air mass flow through the channel is calculated, based on the mean of the measured velocities at the bottom of the channel.

Temperatures in the test rig, as reported henceforward, are taken to be the temperatures above ambient. The inlet temperature is also taken as ambient temperature.

It is further assumed that the width of the channel, 92.5 cm, is sufficient that edge effects are largely eliminated at the centre. This width is similar to large-scale test rigs used by other investigators [31,32,38], and most small-scale investigations had similar height-to-width ratios. Therefore, the conditions measured at the centre line of the test rig are taken to be representative of the conditions in an infinitely wide channel. However, this assumption may be tested in future experiments.

5. Flow rate

The critical performance indicator for the system as a solar chimney is the air flow rate. The flow rate is determined by

$$m = \rho A_x u \tag{1}$$

Fig. 4 shows the flow rate of air through the channel according to the channel depth at different heat inputs. Although the measured data show velocity decreasing with increasing channel depth, the mass flow rate increases with channel depth, and also with heat input.

The dependence of flow rate on the heat input and channel depth can be characterised by the relationship:

$$Re(s) = a(Ra^*)^{\mathrm{b}}\left(\frac{s}{H}\right)^{\mathrm{c}} \tag{2}$$

where the mass flow rate is represented by the Reynolds number:

$$Re(s) = \frac{us}{\nu} \tag{3}$$

and the heat input is represented by the modified Rayleigh number:

$$Ra^* = \frac{g\beta q_{\mathrm{in}} H^4}{\nu^2 k} Pr \tag{4}$$

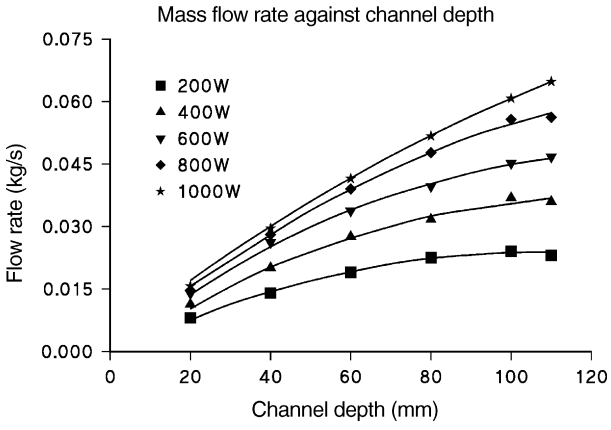

Fig. 4. Mass flow rate against channel depth.

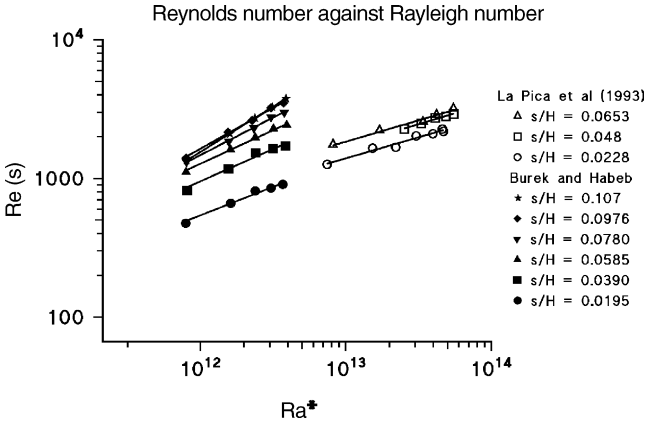

Fig. 5. Variation of Reynolds number with Rayleigh number.

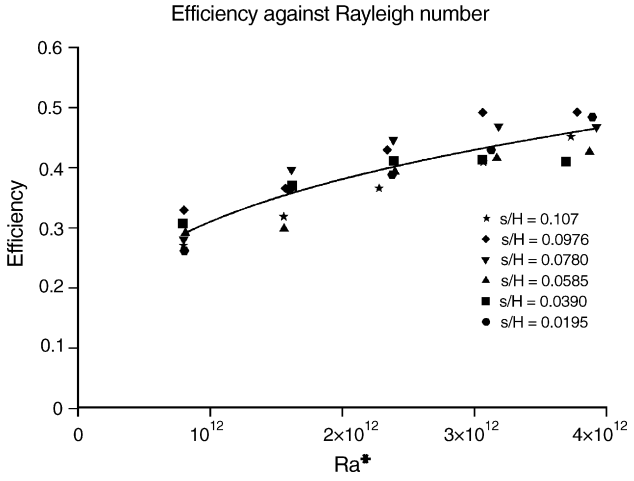

Fig. 6. Variation of thermal efficiency with Rayleigh number.

The other independent variable, i.e., the channel depth, is represented by the aspect ratio (s/H). The properties of air are evaluated at the input temperature.

The result of a multivariate regression analysis, carried out using SigmaPlot software, gives:

$$Re(s) = 0.00116(Ra^*)^{0.572}\left(\frac{s}{H}\right)^{0.712} \quad (5)$$

Statistics for the regression analysis show—correlation coefficient R^2: 0.994; mean percentage error of the data from the calculated regression line: 4.6%; constant $a = 1.16 \times 10^{-3}$: standard error 6.83×10^{-4} (t-ratio 1.70); index for Ra^* 0.572: standard error 0.0218 (t-ratio 26.2); index for s/H 0.712: standard error 0.0242 (t-ratio 29.5).

As a measure of the confidence in the regression coefficient, the absolute value for the t-ratio should be greater than 2. A value of 1.70 for the multiplier constant a indicates uncertainty, but the t-ratios for the indices for Ra^* and s/H indicate confidence in the dependence of the Reynolds number on these parameters, as calculated. Fig. 5 shows Re plotted against Ra^*, and the dependence on s/H is clear to see.

6. Heat output and heat gain efficiency

In terms of a solar collector, the final heat gain and thermal efficiency are of principal interest. Given the temperature rise through the test rig and the flow rate, as measured at the bottom of the test rig, the heat gain is given by

$$Q_o = mc_p(T_o - T_i) \quad (6)$$

The heat gain efficiency is given by

$$\eta = \frac{Q_o}{Q_i} \quad (7)$$

Efficiency can be characterised as a function of heat input and channel depth, using the same form as above for Reynolds number. The results of this analysis, using SigmaPlot, gives:

$$\eta = 8.83 \times 10^{-5}(Ra^*)^{0.298}\left(\frac{s}{H}\right)^{0.0203} \quad (8)$$

Statistics for the regression analysis show—correlation coefficient R^2: 0.824; mean percentage error of the data from the calculated regression line: 6.3%; constant $a = 8.83 \times 10^{-5}$: standard error 7.03×10^{-5} (t-ratio 1.26); index for Ra^* 0.298: standard error 0.0284 (t-ratio 10.5); index for s/H 0.0203: standard error 0.0236 (t-ratio 0.858).

Once again, these results show some uncertainty in the value of the multiplier constant a. However, the thermal efficiency is a strong function of, and correlates well against, the Rayleigh number (i.e., heat input), but it is a very weak function of the channel depth. Fig. 6 shows efficiency plotted against Rayleigh number, and the data points are clustered according to the heat input. At first sight, it appears that there is a trend within each of these clusters, but closer inspection reveals that there is no trend according to channel depth, which in agreement with the regression analysis above.

7. Discussion

The system tested in this set of experiments was built to resemble the essential characteristics of a solar collector, in particular the input is a uniform heat flux (UHF) and it has a transparent cover, through which it loses heat. In this very important way it differs from most other investigations of buoyancy-driven airflow through asymmetrically heated ducts. The case of uniform wall temperature (UWT) – such as reported in [1,8,9] among others – never occurs in practical solar energy applications. Most previous UHF investigations (for example [16]), had an opaque or adiabatic cover (non-heated wall). This may be the case where natural convection in the channel is induced behind an opaque photovoltaic panel (for example [39]), but never for Trombe Walls, nor for solar chimney systems which have a transparent cover. In particular, with an adiabatic non-heated wall, all the heat generated by the heated surface is transferred into the air stream, and therefore the thermal efficiency, by definition, is 100%. Some large-scale experiments on solar applications are based on outdoor test rigs (for example [26,27]), and therefore the heat input is not controllable.

There is a scarcity of data from closely controlled experiments from large-scale test rigs resembling solar collectors, and the data and results from this investigation should be viewed in this context. Of those investigations which have been reported: Bouchair [30] used a symmetrically heated channel; Chen et al. [32] does not present results for Reynolds number and thermal efficiency, and La Pica's test rig [31] has crucial differences compared with the present one.

7.1. Air flow rate

Whilst the general result, that flow rate increases with heat input and with channel depth, might be expected, Bouchair [30] observed that for greater channel depths (between 300 and 500 mm) the flow rate decreases as channel depth increases. The data shown in Fig. 4 do show a small decrease in flow rate at low heat inputs, as the channel depth increases from 100 to 110 mm. Bouchair used a test rig 2.0 m high, and consequently depth-to-height aspect ratios up to 0.25, compared with aspect ratios up to 0.107 in the current experiments. Nevertheless, whilst the slightly decreasing trend from the current data could be due to experimental uncertainties, it might, on the other hand, it support Bouchair's observations and the notion of an optimum channel depth. This may be a topic for future study.

Processing the data presented by La Pica et al. [31] in the same way as the velocity data above, the following relationship is obtained:

$$Re(s) = 0.350(Ra^*)^{0.318}\left(\frac{s}{H}\right)^{0.347} \tag{9}$$

The results are not directly comparable, because of differences in the test rigs, in particular:

- The height of the test rig used in the current investigation was 1.025 m, as opposed to 2.6 m reported by La Pica.
- The cover of the current test rig was transparent plastic sheet, while La Pica used silvered glass.

Furthermore, unlike La Pica's set-up, the test rig in this investigation does not have inlet and outlet ducts, which would affect the airflow through the system. However, the present test rig may be considered as the simplest 'base case', to which such refinements could be added. Nevertheless, the relationship in Eq. (9) is plotted in Fig. 5, and despite all the differences, there appears to be some continuity between the two data sets.

7.2. Thermal efficiency

The power-law relationship between efficiency and heat input suggests that efficiency continues to increase, and therefore it can reach values over 100%. This is clearly impossible. However, for flat-plate solar collectors, the heat input does not normally exceed about 1000 W/m^2 in practical situations. Therefore, the relationship derived above can be regarded as valid for the system considered as a solar collector.

For solar collectors, the heat balance equation is often used to characterise the thermal performance (see, for example [37]):

$$\eta = F_R\left(\tau\alpha - U_L\frac{T_i - T_a}{I}\right) \tag{10}$$

The heat removal factor, F_R, is a function of mass flow rate, and for active (fan-driven) systems, it is considered a constant (to a first-degree approximation). However, for passive (buoyancy-driven) systems, flow rate is a function of the heat input, and therefore not constant, which means that F_R is not constant either. For this set of experiments, in terms of Eq. (10):

- the inlet temperature is equal to the ambient temperature ($T_i = T_a$), and
- $\tau\alpha = 1$, because the heat is supplied by a heating mat behind the absorber plate.

Therefore, Eq. (10) reduces to:

$$\eta = F_R \tag{11}$$

For active systems, with a given constant flow rate, the maximum efficiency is equal to $F_R\tau\alpha$, which is constant irrespective of the heat input. This set of experiments confirms that, for passive systems, F_R is not constant, and shows that the maximum efficiency of the system is dependent on the heat input, and therefore not constant under a given set of practical operating conditions, where the solar input varies throughout the day.

The thermal efficiency depends on the nature of the cover. The principal source of inefficiencies in a solar collector is the heat loss through the cover. The heat loss in turn affects the mass flow rate, and therefore the thermal characteristics of the cover are crucial to the performance of such a system, either as a solar collector or as a solar chimney. This may be a topic for future investigation.

Although the test rig is well-insulated at the back, it is inevitable that there are some heat losses via this route. These have not been measured accurately, but they are estimated to be small compared with the losses via the front cover.

The result that the thermal heat gain and efficiency are independent of channel depth suggests that the thermal boundary layers on the heating plate and the cover are independent of each other—the thermal boundary layers are not fully developed. An analysis presented by Wirtz and Stutzman [40] suggests that, based on [2], for a 20 mm channel depth and 200 W/m^2 input, the thermal boundary layers should merge at about 4.5 m height. Nevertheless, Wirtz and Stutzman also present interferometer images which show that the thermal boundary layers are not entirely independent much lower in the channel. This is linked to the 'chimney effect', whereby although the momentum boundary layers are relatively thin for a single plate, the air is drawn upwards throughout the entire channel depth. The present results are in agreement with Wirtz and Stutzman, namely that although the thermal boundary layers are thin enough to have little effect on the overall heat

gain, the air in the channel away from the boundary layers is nevertheless heated.

The test rig, as described, is thermally lightweight compared with a Trombe Wall construction, which is a very common application of passive systems of this type. Trombe Walls comprise a massive thermal store, whereas the test rig in this investigation had lightweight insulation behind the heated plate. Nevertheless, it still took several hours for the test rig to achieve steady state—a thermally massive Trombe Wall construction would take significantly longer, and indeed, because it is designed to store heat for several hours, and its mode of operation is essentially always transient. Transient performance and the effects of thermal mass are the subject of continuing investigations.

8. Conclusions

The data from this investigation yield some insights into the performance of solar chimneys and passive solar collectors, by varying the heat input and channel depth in a test rig resembling a passive solar collector, approximately 1 m^2. The following are the main conclusions from this investigation:

- The mass flow rate within the channel depends on both the heat input and the channel depth. The current investigation suggests that:

$$m \propto Q_i^{0.572} \ (m \text{ is proportional to } Q_i^{0.572}) \tag{12}$$

and

$$m \propto s^{0.712} \ (m \text{ is proportional to } s^{0.712}) \tag{13}$$

However, other workers' results (for example Bouchair [30]) suggest that there may be an optimum channel depth, which may depend on heat input, to give maximum flow rate. Data from the current investigation for low heat inputs at high aspect ratios show some support for this assertion.

- The efficiency of the system, operating as a passive solar air-heating collector, is dependent on the heat input. For heat inputs up to 1000 W/m^2, the data give the following relationship:

$$\eta \propto Q_i^{0.298} \ (\eta \text{ is proportional to } Q_i^{0.298}) \tag{14}$$

The depth of the channel does not affect the thermal efficiency or the heat output.

This investigation is being continued:

- The current results are based only on one height of channel. Further experiments are being undertaken using channels of different heights to assess the effect of this parameter.
- Temperature and velocity data within the test rig, as it heats up and cools down, are being analysed to assess the transient behaviour of the system.

In a practical system operating as s solar collector, the inlet and outlet would be connected to a room via some kind of duct. Also, the inlet temperature would be different to the ambient temperature. The effect of these parameters on the performance of the system should also be investigated more closely.

References

[1] W. Elenbaas, Heat dissipation of parallel plates by free convection, Physica 9 (1) (1942) 1–24.
[2] W. Aung, L.S. Fletcher, V. Sernas, Developing laminar free convection between vertical flat plates with asymmetric heating, International Journal of Heat and Mass Transfer 15 (1972) 2293–2308.
[3] E.K. Levy, P.A. Eichen, W.R. Cintani, R.R. Shaw, Optimum plate spacing for laminar natural convection heat transfer from parallel vertical isothermal flat plates: experimental verification, Transactions of ASME, Journal of Heat Transfer 97 (1975) 474–476.
[4] L.F.A. Azevedo, E.M. Sparrow, Natural convection in a vertical channel vented to the ambient through an aperture in the channel wall, International Journal of Heat and Mass Transfer 29 (6) (1986) 819–830.
[5] B.W. Webb, D.P. Hill, High Rayleigh number laminar natural convection in an asymmetrically heated vertical channel, Transactions of ASME, Journal of Heat Transfer 111 (1989) 649–656.
[6] N. Onur, M.K. Aktaş, An experimental study on the effect of opposing wall on natural convection along an inclined hot plate facing downward, International Communication Heat Mass Transfer 25 (3) (1998) 389–397.
[7] M.A. Habib, S.A.M. Said, S.A. Ahmed, A. Asghar, Velocity characteristics of turbulent natural convection in symmetrically and asymmetrically heated vertical channels, Experimental Thermal and Fluid Science 26 (2002) 77–87.
[8] E.M. Sparrow, L.F.A. Azevedo, Vertical-channel natural convection spanning between the fully-developed limit and the single-plate boundary-layer limit, International Journal of Heat and Mass transfer 28 (10) (1985) 1847–1857.
[9] J.R. Bodoia, J.F. Osterle, The development of free convection between heated vertical plates, Transactions of ASME, Journal of Heat Transfer 84 (1962) 40–44.
[10] W. Aung, Fully developed laminar free convection between vertical plates heated asymmetrically, International Journal of Heat and Mass Transfer 15 (1972) 1577–1580.
[11] S.H. Kim, N.K. Anand, W. Aung, Effect of wall conduction on free convection between asymmetrically heated vertical plates: uniform wall heat flux, International Journal of Heat and Mass Transfer 33 (5) (1990) 1013–1023.
[12] E.M.A. Mokheimer, Spreadsheet numerical simulation for developing laminar free convection between vertical parallel plates, Computerised Methods Applied Mechanical Engineering 178 (1999) 393–412.
[13] H. Akbari, T.R. Borgers, Free convection laminar flow within the trombe wall channel, Solar Energy 22 (1979) 165–174.
[14] T.R. Borgers, H. Akbari, Free convection turbulent flow within the Trombe Wall channel, Solar Energy 33 (3/4) (1984) 253–264.
[15] F. Mootz, J.-J. Bezian, Numerical study of a ventilated façade panel, Solar Energy 57 (1) (1996) 29–36.
[16] A.G. Fedorov, R. Viskanta, Turbulent natural convection heat transfer in an asymmetrically heated, vertical parallel-plate channel, International Journal of Heat and Mass Transfer 40 (16) (1997) 3849–3860.
[17] A.M. Rodrigues, A. Canha da Piedale, A. Lahallec, J.Y. Grandpeix, Modelling natural convection in a heated vertical channel for room ventilation, Building and Environment 35 (2000) 455–469.
[18] W. Ding, Y. Hasemi, T. Yamada, Natural ventilation performance of a double-skin façade with a solar chimney, Energy and Buildings 37 (4) (2005) 411–418.
[19] S.J. Ormiston, G.D. Raithby, K.G.T. Hollands, Numerical predictions of natural convection in a Trombe Wall, International Journal of Heat and Mass Transfer 29 (6) (1986) 869–877.
[20] R. Letan, V. Dubovsky, G. Ziskind, Passive ventilation and heating by natural convection in a multi-storey building, Building and Environment 38 (2) (2003) 197–208.
[21] K.S. Ong, A mathematical model of a solar chimney, Renewable Energy 28 (2003) 1047–1060.

[22] K.S. Ong, C.C. Chow, Performance of a solar chimney, Solar Energy 74 (2003) 1–17.
[23] C. Balocco, A simple model to study ventilated facades energy performance, Energy and Buildings 34 (2002) 469–475.
[24] D. Infield, L. Mei, U. Eicker, Thermal performance estimation for ventilated PV facades, Solar Energy 76 (2004) 93–98.
[25] N.K. Bansal, M.S. Sodha, S. Ram, S.P. Singh, Evaluation of complex heat transfer coefficients for passive heating concepts, Building and Environment 22 (4) (1987) 259–268.
[26] J. Hirunlabh, W. Kongduang, P. Namprakai, J. Khedari, Study of natural ventilation of houses by a metallic solar wall under tropical climate, Renewable Energy 18 (1999) 109–119.
[27] M. Sandbergh, B. Moshfegh. Investigation of fluid flow and heat transfer in a vertical channel heated from one side by PV elements. Part II. Experimental Study, Proc. World Renewable Energy Congress (WREC), 1996.
[28] C. Afonso, A. Oliveira, Solar chimneys: simulation and experiment, Energy and Buildings 32 (2000) 71–79.
[29] C.J. Hocevar, R.L. Casperson, Thermocirculation data and instantaneous efficiencies to Trombe Walls, in: Proceedings of the Fourth National Passive Solar Conference, Kansas City, Missouri, USA, (1979), pp. 163–167.
[30] A. Bouchair, Solar chimney for promoting cooling ventilation in southern Algeria, Building Services Engineering Research and Technology 15 (2) (1994) 81–93.
[31] A. La Pica, G. Rodono, R. Volpes, An experimental investigation on natural convection of air in a vertical channel, International Journal of Heat and Mass Transfer 36 (3) (1993) 611–616.
[32] Z.D. Chen, P. Bandopadhayay, J. Halldorsson, C. Byrjalsen, P. Heiselberg, Y. Li, An experimental investigation of a solar chimney model with uniform heat flux, Building and Environment 38 (2003) 893–906.
[33] S.A.M. Burek, B. Norton, Performance characterisation of front pass thermosyphoning air panels, International Journal of Ambient Energy 14 (1) (1993) 3–16.
[34] A.A. Habeb. Air flow and heat transfer in passive solar collectors. MPhil Thesis, Glasgow Caledonian University, 2003.
[35] M. Miyamoto, Y. Katoh, J. Kurima, H. Sasaki, Turbulent free convection heat transfer from vertical parallel plates, in: Proceedings of the Eighth International Heat Transfer Conference, vol. 4, San Francisco, (1986), pp. 1593–1598.
[36] L. Kempe. Heat transfer modeling, MSc Thesis, Glasgow Caledonian University, 1999.
[37] J.A. Duffie, W.A. Beckman, Solar Engineering of Thermal Processes, Wiley/Interscience Publication, U.S.A., 1991.
[38] P.H. Nguyen, P. Yerro, J.L. Bernard, P. Sellito, M. Dupont, Wall temperature experimental investigation in a thermally driven channel, Renewable Energy 19 (2000) 443–456.
[39] B. Moshfegh, M. Sandbergh, Flow and heat transfer in the air gap behind photovoltaic panels, Renewable and Sustainable Energy Reviews 2 (1998) 287–301.
[40] R.A. Wirtz, R.J. Stutzman, Experiments on free convection between vertical plates with symmetric heating, Transactions of ASME, Journal of Heat Transfer 104 (1982) 501–507.